Electron Magnetic Resonance Study of the Photoreduction of Alkylviologens in Anionic Sodium Dodecyl Sulfate and Cationic Dodecyltrimethylammonium Bromide Micelles

Don Keun Lee, Yeong Il Kim, Young Soo Kwon,† and Young Soo Kang*

Department of Chemistry, Pukyung National University, Pusan 608-737, Korea

Larry Kevan*

Department of Chemistry, University of Houston, Houston, Texas 77204-5641

Received: July 23, 1996; In Final Form: November 11, 1996[⊗]

Photoinduced electron transfer from micellar counterions to a viologen moiety through the micellar interface was studied versus the pendant alkyl chain length, the number of alkyl chains on the viologens, and the interface charge of the micelles. The photoreduction yields decrease more rapidly with increasing alkyl chain length for dialkylviologens than for monoalkylviologens due to greater hydrophobic interactions with the surfactant alkyl chains. This also results in higher photoyields of the monoalkylviologens versus the dialkylviologens due to a shorter electron transfer distance for the monoalkylviologens even though the dialkylviologens have better coupling with the micellar counterions due to an orientation of the viologen moiety parallel to the micellar interface. Larger photoyields are obtained in cationic dodecyltrimethylammonium bromide (DTAB) micelles than in anionic sodium dodecyl sulfate (SDS) micelles because of a lower energy barrier for electron transfer through the positively charged micellar interface. Thus, photoinduced electron transfer across micellar interfaces is controlled first by the energy barrier, second by the electron-transfer distance, and third by the relative orientations of the donor and acceptor.

Introduction

Molecular assemblies such as micelles, reverse micelles, and vesicles have been used as model systems for light energy conversion into chemical energy and its storage.[1−4] Such molecular assemblies can compartmentalize the electron transfer process across an interface between an electron donor and acceptor. This enhances the charge separation when there is an interface charge. Controlling the interface charge permits control of the energy barrier for electron transfer through the interface to optimize the net charge separation by suppressing back electron transfer.

Photosensitive materials such as ruthenium complexes,[5] chlorophylls,[6,7] porphyrins,[8−10] and phenothiazines[11−16] have been studied to achieve photoinduced charge separation within molecular assemblies to enhance charge separation yields. Viologens have been intensively studied because of a long lifetime and high photoreduction yields.[17−29] Viologens are easily solubilized into molecular assemblies. Control of the electron transfer distance from the interface to the viologen is possible by attaching variable length alkyl chains to the viologens which then penetrate variously into molecular assemblies. The photoproduced radicals can be characterized by optical absorption, electron spin resonance (ESR), and electron spin echo modulation (ESEM).

ESR has been used to investigate the quantitative yield trends of photoreduction and to identify the radical species.[30,31] ESR also gives information about the microenvironment of the radical surroundings. ESEM measures relative distance differences between a photoreduced viologen radical and the surfactant assembly interface defined by deuterated water by measuring the deuterium modulation depth.[4,32]

In this study the photoreduction yields of alkylviologens are studied in terms of geometrical orientation control of the viologen moiety with respect to the micellar interface. This is carried out by a comparison between monoalkyl- and dialkylviologens with different alkyl chain lengths. Different geometrical orientations of the viologen moiety are expected to result in different electron-transfer distances from the interface and different electronic couplings between the micellar counterions and the viologens. The photoreduction yield is determined by double integration of the ESR spectra. The location of the viologen moiety from the micellar interface is measured by the deuterium modulation depth from ESEM.

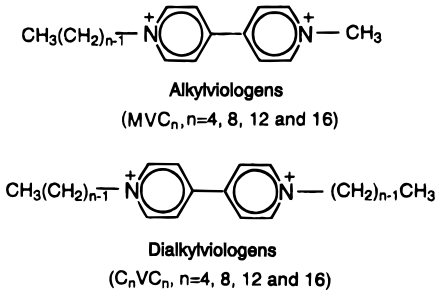

Figure 1. Structures of alkylviologens (MVC_n) and dialkylviologens (C_nVC_n).

Experimental Section

Materials. Sodium dodecyl sulfate (SDS), 4,4′-dipyridyl, and deuterium oxide (D_2O, 99.9 atom % D) were purchased from Aldrich Chemical Co. Dodecyltrimethylammonium bromide (DTAB) was purchased from Eastman Kodak. The micelle forming surfactants were recrystallized three times from ethanol and washed with ethyl ether, followed by drying at 50 °C under a moderate vacuum. Stock micellar solution of 0.1 M SDS and DTAB were prepared in deoxygenated deuterium oxide. Alkylviologen dichlorides (MVC_n, $n = 4, 8, 12, 16$) and dialkylviologen dichlorides (C_nVC_n, $n = 4, 8, 12, 16$) (Figure 1) were prepared by the procedures previously reported.[33] Stock solu-

† Department of Electrical Engineering, Dong-A University, Pusan 604-714, Korea.

[⊗] Abstract published in *Advance ACS Abstracts,* June 15, 1997.

S1089-5647(96)02221-3 CCC: $14.00

tions of 10 mM alkylviologens were prepared in chloroform, and equivalent concentrations of dialkylviologen solutions were prepared in a minimum amount of methanol and then diluted with chloroform to the desired concentration.

Sample Preparation. A 70 μL quantity of the viologen stock solutions was transferred into a 16 mm i.d. by 125 mm long Fisher test tube. The solvent was evaporated under a stream of pure nitrogen. This resulted in the formation of a thin film on the test tube wall. After the film had formed, 1 mL of a 0.1 M stock micellar solution was added to the test tube. The resulting suspensions were sonicated for 5 min at 45 $\pm$ 3 °C with a Fisher Model 300 sonic dismembrator operated at 35% relative output power through a 4 mm o.d. microtip under a nitrogen atmosphere to obtain a clear solution. The exact viologen concentration of the resulting micellar aqueous suspension was measured as 5.98×10^{-4} M by optical absorption spectroscopy. Following equilibration, a portion of the 100 μL solution was placed into separate Suprasil quartz tubes (3 mm o.d. by 2 mm i.d.) which were flame-sealed at one end for photolysis and electron magnetic resonance experiments. The tubes were shaken to equilibrate the solution, and then the samples were frozen by rapidly plunging into liquid nitrogen. Since micelles retain their shape in frozen solutions, the information provided by electron magnetic resonance spectroscopies in frozen solutions provides insight into the structural features of the molecular assemblies at room temperature.[30]

Photolysis. Photoirradiation of the frozen samples was carried out for 10 min at 77 K in a 50 mL quartz Dewar (Wilmad Glass Co.) with a 300 W Cermax xenon lamp (LX300 UV). The power supply (ILC Technology) was operated at 50% (10 A) of its rated maximum output power. During photolysis the Dewar was rotated at 4 rpm to ensure even irradiation of the sample. The irradiation light passed through a filter combination (10 cm water filter and a Corning glass filter, No. 7-54), which passed light at the maximum absorbance of methylviologen (MV^{2+}, $\lambda_{max} = 257$ nm[34]). The alkylviologens have the same λ_{max} and about the same extinction coefficient. By use of a YSI Kettering Model 65 radiometer, the average radiant power incident upon the sample was determined as 1.0×10^3 W m^{-2}. After photoirradiation, the sample tubes were stored in liquid nitrogen.

Electron Magnetic Resonance and Data Manipulations. ESR spectra were recorded at X-band with a Bruker ESP 300 spectrometer with 100 kHz field modulation. The sample was irradiated at 77 K in one Dewar and transferred to a 200 mL quartz ESR Dewar (Wilmad Glass Co.) containing liquid nitrogen which was then inserted into a TE_{102} cavity. This step eliminated background signals from the irradiation Dewar. The microwave power level was maintained at 0.197 mW to avoid power saturation, and the frequency was measured with a Hewlett-Packard 5350B frequency counter. The magnetic field was monitored with a Bruker ER 032M Hall effect field controller. The standard spectrometer settings used in the ESR experiments were 0.272 mT modulation field amplitude, 20 mT sweep width, 9 scan accumulations, 42 s scan time, 0.164 s time constant, 9.511 GHz microwave frequency, and 1.25×10^5 receiver gain. A typical signal-to-noise ratio for the ESR spectra recorded with these settings was 120:1. The viologen radical photoyield was determined by numerical integration of each of the ESR spectra using the ESP 1600 software. Normalized photoyields for the radicals produced by photoirradiation were obtained by dividing by the highest yield for *N*-methyl-*N*′-butylviologen (MVC_4) in DTAB/D_2O micelles.

Two-pulse electron spin echo (ESE) signals were recorded at 4.2 K with a home-built electron spin echo spectrometer which was operated at X-band.[32] The microwave frequency incident upon the sample was measured with a Hewlett-Packard 5342A microwave frequency counter, and the magnetic field was monitored with a Varian F501 gaussmeter. The microwave pulse sequences and data acquisition processes were controlled by a Nicolet 12/80 minicomputer which was interfaced to the ESE spectrometer. Typical microwave pulse widths used in these experiments were 40 and 80 ns for $\pi/2$ and π pulses. Once obtained, the ESE data were transferred to an IBM-compatible 586 based microcomputer for later, off-line analysis. The deuterium modulation depths were normalized by dividing the depth at the first modulation minimum by the depth to the base line at the same interpulse time.[30] The simulation of the ESE signal was carried out with ESFT software by fitting to the isotropic coupling constant ($a_{iso} = 0.1$ MHz), the dipolar interaction distance (R), and the number of nuclei interacting with the unpaired electron (N).

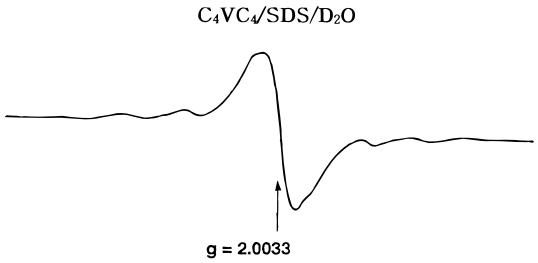

Figure 2. ESR spectra at 77 K of C_4VC_4/SDS/D_2O micelle after 10 min photoirradiation at 77 K.

Results

A photoirradiated sample without alkylviologens or dialkylviologens showed no ESR signal. This indicates that the viologens are the photosensitive material in these systems. The intensity of the ESR signal reached a plateau after 10 min photoirradiation. Figure 2 shows the ESR spectra of C_4VC_4 in SDS micelles after 10 min photoirradiation. The viologen radical is identified with $g = 2.0033$ and a violet color after photoirradiation. More than one radical is present due to radical conversion from the viologens to the alkyl chain of the surfactants. Radical conversion during photolysis has been reported in previous studies.[22] Radical conversion from a viologen radical to a surfactant alkyl radical is indirectly indicated by a maximum violet color after 10 min photoirradiation. A decreasing violet color with increasing photoirradiation time after 10 min is caused by radical conversion from the viologen radical ion to surfactant alkyl chains.

The normalized photoyields of alkylviologens and dialkylviologens in SDS/D_2O micelles are shown in Figure 3. The photoyields of the alkylviologens decrease monotonically with increasing alkyl chain length. The photoyields of the dialkylviologens decrease less. Thus, alkylviologens show higher photoyields than dialkylviologens.

The normalized deuterium modulation depths of alkylviologens and dialkylviologens in SDS/D_2O micelles are shown in Figure 4. The deuterium modulation depths of the alkylviologens are higher than those of the dialkylviologens. The deuterium modulation depths of the alkylviologens monotonically decrease with increasing alkyl chain length. The deuterium modulation depths of the dialkylviologens only slightly decrease with increasing alkyl chain length.

The normalized photoyields of the alkylviologens and dialkylviologens in DTAB/D_2O micelles are shown in Figure 5. The photoyields of the alkylviologens decrease with increasing alkyl chain length. The photoyields of the dialkylviologens only

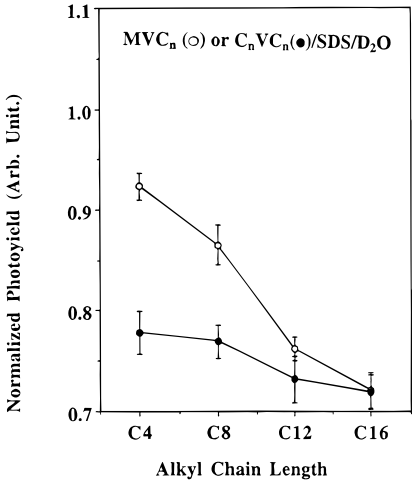

Figure 3. Normalized photoyields at 77 K of MVC_n (○) and C_nVC_n (●) in SDS/D_2O micelles versus the C_n alkyl chain length after 10 min photoirradiation at 77 K.

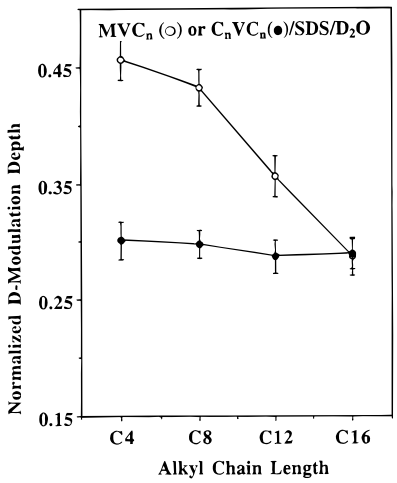

Figure 4. Normalized modulation depths at 4.2 K of MVC_n (○) and C_nVC_n (●) in SDS/D_2O micelles versus the C_n alkyl chain length after 10 min photoirradiation at 77 K.

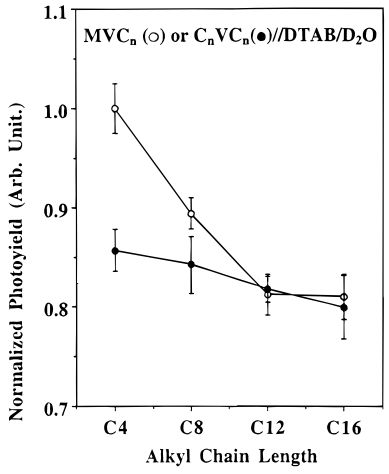

Figure 5. Normalized photoyields at 77 K of MVC_n (○) and C_nVC_n (●) in $DTAB/D_2O$ micelles versus the C_n alkyl chain length after 10 min photoirradiation at 77 K.

slightly decrease with increasing alkyl chain length. The alkylviologens have higher photoyields than the dialkylviologens in $DTAB/D_2O$ micelles. The photoyields of the alkylviologens decrease more rapidly with alkyl chain length than those of the dialkylviologens.

The normalized deuterium modulation depths of the alkylviologens and the dialkylviologens in $DTAB/D_2O$ micelles are shown in Figure 6. The deuterium modulation depths of the alkylviologens decrease more rapidly with increasing alkyl chain length. The deuterium modulation depths of the dialkylviologens only slightly decrease with increasing alkyl chain length. Higher deuterium modulation depths are obtained from the alkylviologens than from the dialkylviologens.

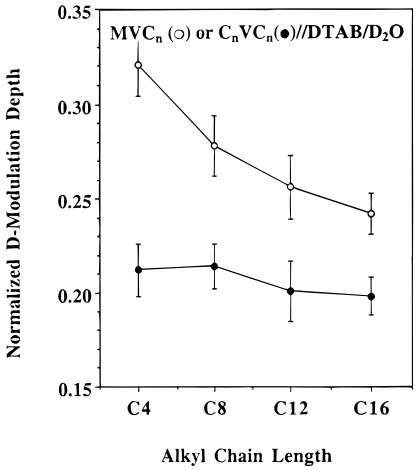

Figure 6. Normalized modulation depths at 4.2 K of MVC_n (○) and C_nVC_n (●) in $DTAB/D_2O$ micelles versus the C_n alkyl chain length after 10 min photoirradiation at 77 K.

The photoyields of the alkylviologens and the dialkylviologens are higher in $DTAB/D_2O$ micelles than in SDS/D_2O micelles. On the other hand, the deuterium modulation depths of alkylviologens and dialkylviologens are higher in SDS/D_2O micelles than in $DTAB/D_2O$ micelles.

Discussion

The orientation of the electron donor and electron acceptor, the electron-transfer distance between donor and acceptor, the free energy of the electron-transfer reaction, and the degree of electronic coupling are critical parameters for photoinduced electron transfer. The effect of the electron-transfer distance between donor and acceptor, the free energy of electron transfer, and the degree of electronic coupling have been studied experimentally.[4−31,35−37] Theoretical studies on orientation effects in electron transfer have been reported.[38−41] The orientation of the electron donor and acceptor can affect the degree of electronic coupling between them.

In previous studies[5−30] photoinduced electron transfer through molecular assembly interfaces was studied by varying the electron transfer distance between the donor and acceptor by adding a pendant alkyl chain to either and by varying the electron transfer energy by changing the interface charge. The photoinduced electron transfer efficiency exponentially decreases with increasing transfer distance and is also decreased by changing the interface charge from positive to neutral or negative.

A previous study[25] reported that the photoreduction of viologens occurs by electron transfer from the viologen dichloride counterions or from the SDS or DTAB surfactant headgroups. In the present study, the photoreduction of alkylviologens and dialkylviologens are compared with respect to the electron-transfer distance, the interface charge, and the orientation of the viologen moiety. The orientation of the viologen moiety was varied by attaching one or two pendant alkyl chains to the viologen.

The photoreduced viologen cation radical is identified by its violet color and *g* factor near 2.003. The violet color is greatest

after 10 min irradiation and thereafter decreases with increasing irradiation time. The ESR peak intensities of the viologen radical decrease and those of the surfactant alkyl radical increase with increasing irradiation time. This indicates that the viologen radical is converted into surfactant alkyl radicals with increasing irradiation time as found in other systems.[22,25,29]

The viologen counterions remain at the interface while the viologen ions are solubilized somewhat into the micelles.[25,27,42] The photoproduced quantities of viologen radical and surfactant alkyl radical indicate the net electron-transfer efficiency from the counterion to the viologen moiety through the micellar interface. The relative photoyields are determined by double integration of the ESR signals. These photoyields are normalized by dividing by the highest photoyield value for MVC_4 in DTAB/D_2O micelles. The photoyields of MVC_n in SDS/D_2O micelles monotonically decrease with increasing alkyl chain length of the viologens. The photoyields of C_nVC_n in SDS/D_2O micelles only slightly decrease with increasing alkyl chain length of the viologens. The decrease of photoyield with increasing alkyl chain length of the viologens reflects an increasing electron-transfer distance between the electron donor and acceptor. An increasing alkyl chain length on the viologen increases the hydrophobic interaction of the viologen molecules with the surfactant alkyl chains. This results in a deeper location of the viologen moiety into the hydrophobic core region of the micelles and increases the distance between the counterions and the viologen moiety. Similar results are observed for alkylphenothiazines in micelles and vesicles.[11−13]

Here we focus on the different photoyield trends between alkylviologens and dialkylviologens with increasing alkyl chain length. The number of alkyl chains affects the photoyield for two different reasons. The first effect is that two alkyl chains cause the viologen moiety to penetrate deeper into the hydrophobic core region of the micelle compared to one alkyl chain because of greater hydrophobic interactions. This results in a lower photoyield for dialkylviologens compared to alkylviologens due to a shorter distance between the counterions at the micellar interface and the viologen moiety of the dialkylviologens. The second effect is the greater photoyield decrease with increasing alkyl chain length for alkylviologens than for dialkylviologens This can be explained by different orientations of the viologen moiety in the micelles. Two alkyl chains on a viologen cause the viologen moiety to be about parallel with the micellar interface as shown in Figure 7B. In contrast, one alkyl chain on a viologen causes the viologen moiety to be about perpendicular to the micellar interface as shown in Figure 7A. The greater hydrophobicity of dialkylviologens is less affected by the increased alkyl chain length of the viologens. This results in a lesser photoyield decrease versus alkyl chain length for dialkylviologens versus alkylviologens. The parallel orientation of the viologen moiety for the dialkylviologens theoretically allows greater electronic coupling between the donor and acceptor.[38−41] This should result in a higher photoreduction yield for dialkylviologens versus alkylviologens, which is not observed. Therefore, the higher photoyield of the alkylviologens, even with a perpendicular orientation of the viologen moiety with respect to the micellar interface, indicates that viologen photoreduction is dominated by the electron-transfer distance more than by the orientation of the viologen moiety.

These interpretations are supported by the normalized deuterium modulation depths of the alkylviologens and dialkylviologens in SDS/D_2O micelles as shown in Figure 4. A lower deuterium modulation depth indicates a longer electron transfer distance from the counterion at the micellar interface to the viologen. Greater deuterium modulation depths are obtained

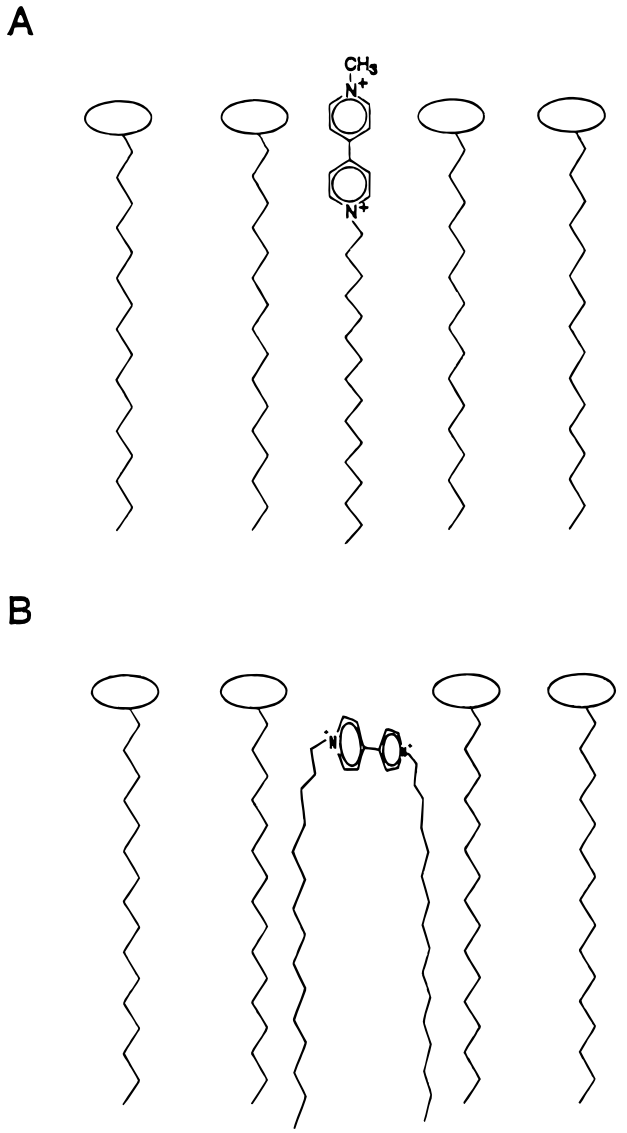

Figure 7. Schematic orientation of the viologen moiety in (A) MVC_n and (B) C_nVC_n with respect to the micellar interface.

from alkylviologens than from dialkylviologens. The deuterium modulation depths of alkylviologens decrease monotonically with increasing alkyl chain length. On the other hand, the deuterium modulation depths of dialkylviologens only slightly decrease with increasing alkyl chain length. The deuterium modulation depths correlate with the photoyield data and support the trend of electron-transfer distance changes. The number of interacting deuterium nuclei (N) and their distance (R) to the viologen radical were determined by ESEM simulation for an isotropic coupling constant of 0.1 MHz.[32] The distance is in the range 2.8−5.6 Å, and the numbers of deuterium nuclei are in the range 9−13. Representative simulated spectra of C_8VC_8 (A) and MVC_4 (B) in SDS/D_2O micelles are shown in Figure 8. The number and distance of interacting deuterium nuclei with the viologen cation radical of C_8VC_8 in SDS/D_2O micelles are 12 and 4.5 Å, respectively. The number and distance of interacting deuterium nuclei with the viologen radical of MVC_8 in SDS/D_2O micelles are 10 and 3.9 Å, respectively.

The same photoyield and deuterium modulation depth trends for C_nVC_n and MVC_n in DTAB/D_2O micelles are also obtained in SDS/D_2O micelles. This means that the alkylviologens and dialkylviologens have different orientations of the viologen moiety and different degrees of hydrophobic interaction with the surfactant alkyl chains in both micellar systems.

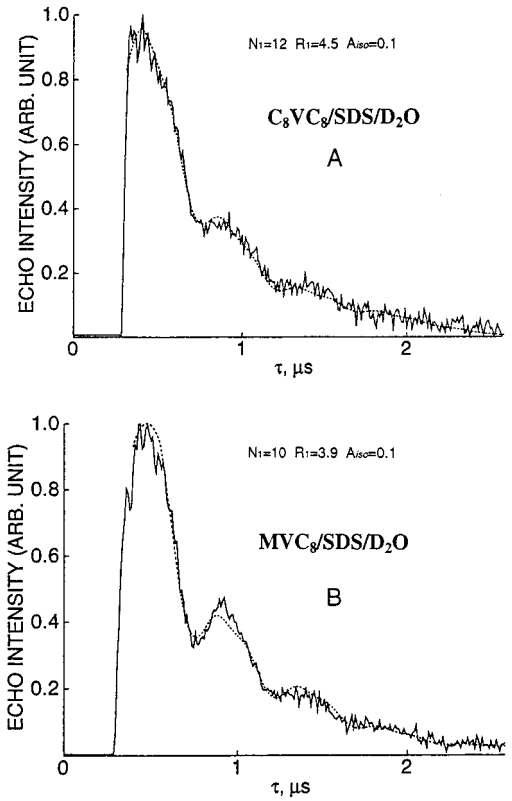

Figure 8. Experimental (—) and simulated (···) two-pulse X-band ESE signals of (A) C_8VC_8 and (B) MVC_8 in SDS/D_2O micelles.

The photoyields of C_nVC_n and MVC_n in $DTAB/D_2O$ micelles are higher than in SDS/D_2O micelles even with lower deuterium modulation depths. This implies that the cationic interface charge of DTAB micelles gives a lower energy barrier for electron transfer than the anionic interface charge of SDS micelles as also found in previous studies.[11−16] The higher photoyields in DTAB micelles than in SDS micelles indicate that electron transfer is dominated more by the energy barrier of the micellar interface than by the electron-transfer distance.

Conclusions

The photoinduced electron-transfer efficiency from counterions at the micellar interface to viologens is controlled by the electron-transfer distance, energy barrier, and orientation of the viologen moiety. The electron-transfer distance increases with the pendant alkyl chain length of the viologen, which decreases the photoyield. The energy barrier to electron transfer through the micellar interface is greater in cationic DTAB micelles than in anionic SDS micelles. The energy barrier associated with the micellar interface charge dominates the differences in the electron-transfer distance. The orientation of the viologen moiety relative to the micellar interface was varied by attaching one or two alkyl chains to the viologens. The number of alkyl chains also results in different degrees of hydrophobic interaction which locates the viologens at different depths into the micellar core. However, the orientation of the viologen moiety is less important than the hydrophobicity effect which varies the electron-transfer distance. Thus, the factors that control the efficiency of photoinduced electron transfer across micellar interfaces are the energy barrier, the electron-transfer distance, and the relative orientations of the donor and acceptor in order of decreasing importance.

Acknowledgment. This research was supported by the Division of Chemical Sciences, Office of Basic Research, Office of Energy Research, U.S. Department of Energy. Y.S. Kang thanks the Korean Research Foundation, Department of Education of the Republic of Korea, and Y. S. Kwon thanks the Korea Electric Power Co. for financial support.

References and Notes

(1) Kalyanasundaram, K. *Photochemistry in Microheterogeneous Systems*; Academic Press: New York, 1987.

(2) Fendler, J. H. *Acc. Chem. Res.* **1980**, *13*, 7.

(3) Hurly, J. K.; Tollin, G. *Sol. Energy* **1982**, *28*, 187.

(4) Kevan, L. In *Photoinduced Electron Transfer, Part B*; Fox, M. A., Chanon, M., Eds.; Elsevier: Amsterdam, 1988; pp 329−384.

(5) Colaneri, M. J.; Kevan, L.; Schmehl, R. *J. Phys. Chem.* **1989**, *93*, 397.

(6) Hiromitsu, I.; Kevan, L. *J. Chem. Phys.* **1988**, *88*, 691.

(7) Hiff, T.; Kevan, L. *Photochem. Photobiol.* **1988**, *48*, 553.

(8) Lanot, M. P.; Kevan, L. *J. Phys. Chem.* **1989**, *93*, 998.

(9) Chastenet de Castaing, E.; Kevan, L. *J. Phys. Chem.* **1991**, *95*, 10178.

(10) Kang, Y. S.; McManus, H. J. D.; Liang, K.; Kevan, L. *J. Phys. Chem.* **1994**, *98*, 1044.

(11) Kang, Y. S.; Baglioni, P.; McManus, H. J. D.; Kevan, L. *J. Phys. Chem.* **1991**, *95*, 7944.

(12) Kang, Y. S.; McManus, H. J. D.; Kevan, L. *J. Phys. Chem.* **1992**, *96*, 10049.

(13) Kang, Y. S.; McManus, H. J. D.; Kevan, L. *J. Phys. Chem.* **1992**, *96*, 10055.

(14) Kang, Y. S.; Kevan, L. *J. Chem. Soc., Faraday Trans.* **1993**, *89*, 1377.

(15) Kang, Y. S.; Kevan, L. *Langmuir* **1993**, *9*, 1691.

(16) Kang, Y. S.; McManus, H. J. D.; Kevan, L. *J. Phys. Chem.* **1992**, *96*, 8647.

(17) Thompson, D. H. P.; Barrette, Jr., W. C.; Hurst, J. K. *J. Am. Chem. Soc.* **1987**, *109*, 2003.

(18) Colaneri, M. J.; Kevan, L.; Thompson, D. H. P.; Hurst, J. K. *J. Phys. Chem.* **1987**, *91*, 4072.

(19) Patterson, B. C.; Thompson, D. H.; Hurst, J. K. *J. Am. Chem. Soc.* **1988**, *110*, 3656.

(20) Patterson, B. C.; Hurst, J. K. *J. Chem. Soc., Chem. Commun.* **1990**, 1137.

(21) Colaneri, M. J.; Kevan, L.; Schmehl, R. *J. Phys. Chem.* **1989**, *93*, 397.

(22) Sakaguchi, M.; Kevan, L. *J. Phys. Chem.* **1989**, *93*, 6039.

(23) Sakaguchi, M.; Kevan, L. *J. Phys. Chem.* **1991**, *95*, 5996.

(24) McManus, H. J. D.; Kevan, L. *J. Phys. Chem.* **1991**, *95*, 10172.

(25) McManus, H. J. D.; Kang, Y. S.; Kevan, L. *J. Phys. Chem.* **1992**, *96*, 2274.

(26) Sakaguchi, M.; Baglioni, P.; Kevan, L. *J. Phys. Chem.* **1992**, *96*, 2272.

(27) McManus, H. J. D.; Kang, Y. S.; Kevan, L. *J. Phys. Chem.* **1992**, *96*, 5622.

(28) Xiang, B.; Kevan, L. *J. Phys. Chem.* **1994**, *98*, 5120.

(29) McManus, H. J. D.; Kang, Y. S.; Kevan, L. *Langmuir* **1994**, *10*, 2613.

(30) Kevan, L. *Int. Rev. Phys. Chem.* **1990**, *9*, 307.

(31) Kevan, L. *Radiat. Phys. Chem.* **1990**, *36*, 181.

(32) Kevan, L. In *Modern Pulsed and Continuous-Wave Electron Spin Resonance*; Kevan, L., Bowman, M., Eds.; Wiley: New York, 1990; Chapter 5.

(33) Pileni, M.-P.; Braun, A. M.; Gratzel, M. *Photochem. Photobiol.* **1980**, *31*, 423.

(34) Watanabe, T.; Honda, K. *J. Phys. Chem.* **1982**, *86*, 1617.

(35) Kakitani, T.; Mataga, N. *J. Phys. Chem.* **1986**, *90*, 993.

(36) Kakitani, T.; Mataga, N. *J. Phys. Chem.* **1987**, *91*, 6277.

(37) Yoshimori, A.; Kakitani, T.; Enomoto, Y.; Mataga, N. *J. Phys. Chem.* **1989**, *93*, 8316.

(38) Isied, S. S.; Ogowa, M. Y.; Wishart, J. F. *Chem. Rev. (Washington, D.C.)* **1992**, *92*, 381.

(39) Wasielewski, M. R. *Chem. Rev. (Washington, D.C.)* **1992**, *92*, 435.

(40) Siders, P.; Cave, R. J.; Marcus, R. A. *J. Chem. Phys.* **1984**, *81*, 5613.

(41) Ohta, K.; Closs, G. L.; Morokuma, K.; Green, N. J. *J. Am. Chem. Soc.* **1986**, *108*, 1319.

(42) Wong, M.; Thomas, J. K.; Nowak, J. *J. Am. Chem. Soc.* **1977**, *99*, 4730.